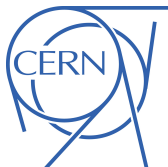


The ATLAS Pixel Detector upgrade from data acquisition to improved track reconstruction for better physics

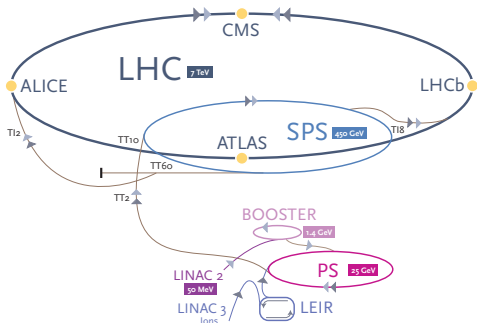
Pierfrancesco Butti (PF)
SLAC Experimental Seminar

February 28, 2019



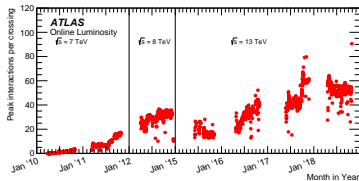
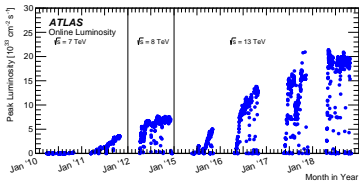
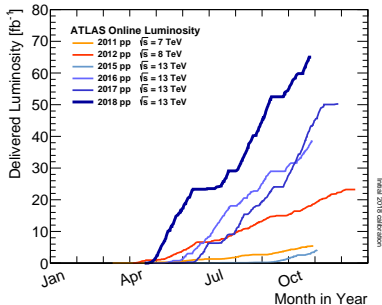
- The LHC Accelerator Complex and ATLAS
- A Supersymmetry search at ATLAS: GMSB $\tilde{t} \rightarrow \tilde{\tau}$
- Final state objects reconstruction
- **From Run-1 to Run-2: some of the challenges from Pixel operation, tracking and Inner Detector Alignment point of view**
- **Run-2 Commissioning and operation**
- Run-2 updates to $\tilde{t} \rightarrow \tilde{\tau}$
- Wrap up

The LHC Accelerator Complex



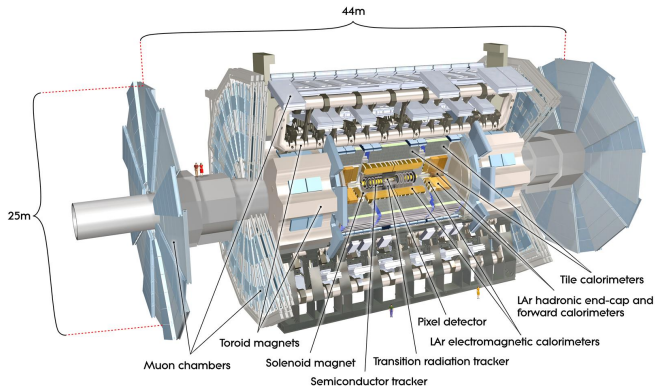
$$N_{pp \rightarrow X} = \mathcal{L} \times \sigma_{pp \rightarrow X}$$

\mathcal{L} = Luminosity (beam params)
 $\sigma_{pp \rightarrow X}$ = process X cross section



The ATLAS Experiment

- General purpose detector at the LHC
- Trigger system L1, L2, EventFilter (Run-1) L1+HLT Farm (Run-2)
- Liquid Argon (EM & Endcap/Forward HCal) and Tile (Barrel HCal) Calorimeters ($|\eta| < 4.9$)
- Muon Spectrometer ($|\eta| < 2.7$)
- Inner Detector ($|\eta| < 2.5$) comprises 3 different technologies
 - Silicon Pixel (Pixel, + IBL from Run-2)
 - Silicon Microstrips (Semiconductor Tracker, SCT)
 - Gaseous Straw Tubes (Transition Radiation Tracker, TRT)

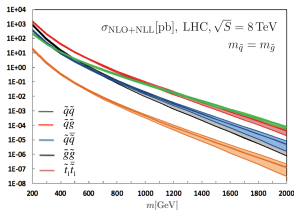


Search for SuperSymmetry (SUSY)

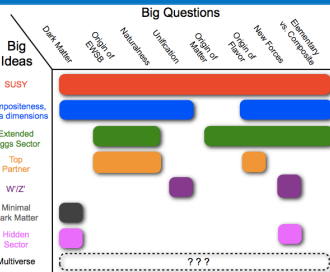
- Standard Model (SM) of elementary particles is a very successful theory
- Completed by the discovery of the Higgs boson in 2012 at LHC by ATLAS and CMS

Some SM Shortcomings:

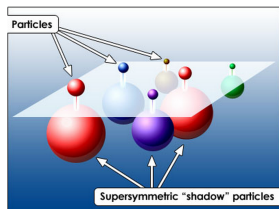
- Dark Matter, Gauge coupling unification, hierarchy problem, matter/anti-matter asymmetry...
- SUSY provides a framework capable to give and answer to each *Big Question***



NLL-Fast



Snowmass '13 meeting

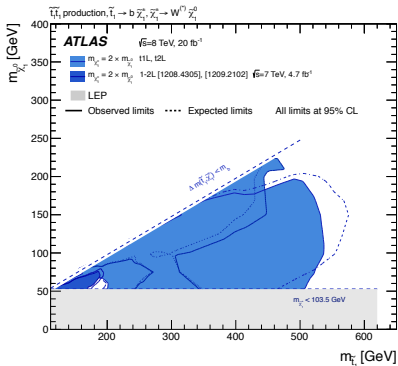
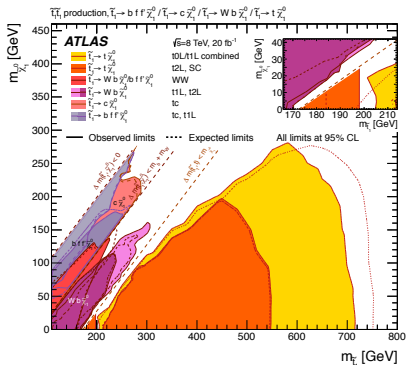


Focused on $\tilde{t}\tilde{t}^*$ search



What was covered back then

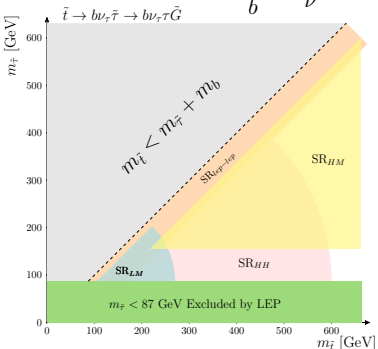
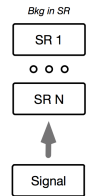
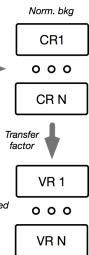
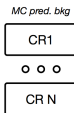
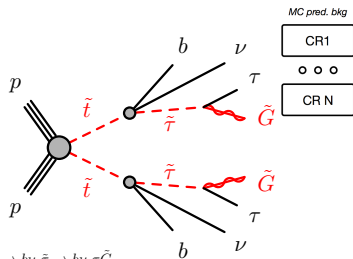
ATLAS Run 1 searches for top squark pair production with χ^0 Least Supersymmetric Particle (LSP)



- Focus on χ^\pm and χ^0 in the decay chain
- Other searches with \tilde{G} as LSP did not include $\tilde{\tau}$ in the decay chain
EPJC, 74, 6, p. 2883 (2014)

- No coverage on final state topologies with hadronically decaying τ particles
- Which possible SUSY scenarios allow for that?

Analysis overview

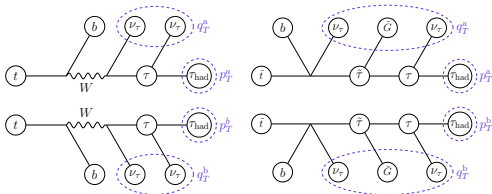


- ## Analyses
- Run-1: Di-Lep JHEP 6, 1-66 (2014)
 - **Run-1: HadHad / LepHad EPJC 76:81 (2016)**
 - Run-2: LepHad / HadHad PRD 98, 032008 (2018)



HH channel - Preselection and Discriminating Variables

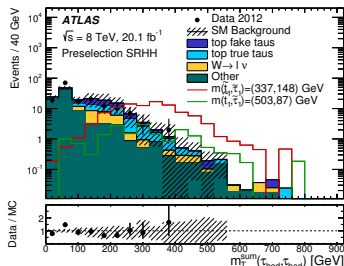
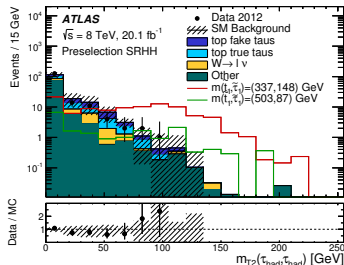
Variable	Cut Value
$N_\mu + N_{el}$	= 0
$N_{\tau_{had}}$	= 2
N_{jets}	≥ 2
$jet_{p_T}^1$	≥ 40 GeV
E_T^{miss}	≥ 150 GeV
$ \Delta\phi(E_T^{miss}, jet_i) $ $i = 1, 2$	≥ 0.5



$$m_T(a, b) = \sqrt{m_a^2 + m_b^2 + 2(E_T^a E_T^b - \mathbf{p}_T^a \cdot \mathbf{p}_T^b)}$$

$$m_{T2}(a, b) = \sqrt{\min_{\mathbf{q}_T^a + \mathbf{q}_T^b = \mathbf{p}_T^{miss}} (\max [m_T^2(\mathbf{p}_T^a, \mathbf{q}_T^a), m_T^2(\mathbf{p}_T^b, \mathbf{q}_T^b)])}$$

$$m_{T2}^{\text{sum}}(\tau_{had}, \tau_{had}) = m_T(\tau_{had,1}) + m_T(\tau_{had,2})$$

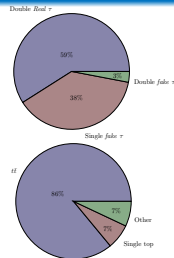


HH channel - Signal Region and Background estimate

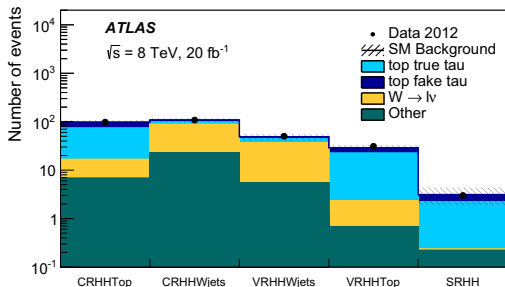
Region	$N_{\tau_{had}}$	N_{μ}	N_{jet}	N_{b-jet}	E_T^{miss}	$\Delta\phi(j_{1,2}, p_T^{miss})$	$m_{T2}(\tau_{had}, \ell)$	$m_T^{sum}(\tau_{had}, \ell)$
SRHH	2	0	≥ 2	≥ 1	> 150 GeV	≥ 0.5	> 50 GeV	> 160 GeV
CRHHTop	1	1	≥ 2	≥ 1	> 100 GeV	≥ 0.5	-	[70, 120] GeV
CRHHWjets	1	1	≥ 2	0	> 100 GeV	≥ 0.5	< 40 GeV	[80, 120] GeV
VRHHTop	1	1	≥ 2	≥ 1	> 120 GeV	≥ 0.5	< 40 GeV	[120, 140] GeV
VRHHWjets	1	1	≥ 2	0	> 120 GeV	≥ 0.5	< 40 GeV	[120, 150] GeV
CRHHQCD	$\geq 2^a$	0	≥ 2	≥ 1	> 150 GeV	$\leq 0.5^b$	-	-

^a For the multi-jet control region (CRHHQCD), no identification criteria are applied to tau leptons

^b The $\Delta\phi$ requirement only applies to the sub-leading jet j_2



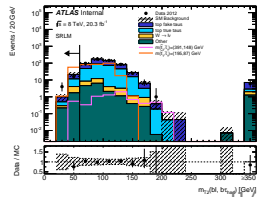
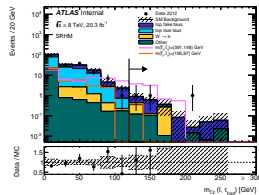
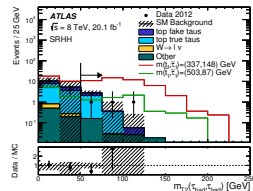
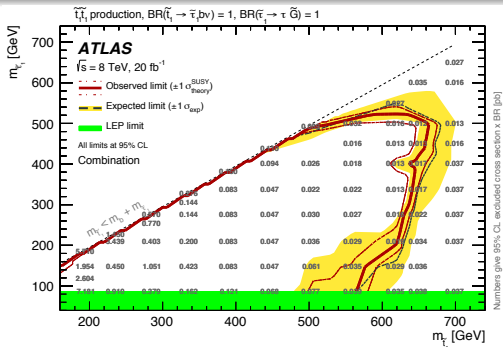
- **Real τ_{had}** : Estimated from MC
- **1 Fake τ_{had}** : Using MC, scaled to observed data in two dedicated CRs
- **2 Fake τ_{had}** : Using MC for ElectroWeak contribution. Data-driven estimate for Multijet background from QCD enriched CR.
- Predictions are tested in specially-designed VRs \rightarrow transfer to SR



Combination with Lep/Had + Lep/Lep and Results

Channel	SRHH	SRLM	SRHM
Observed events	3	20	3
Pre-fit bkg events	3.7	25.8	2.2
Post-fit bkg events	3.1 ± 1.2	22.1 ± 4.7	2.1 ± 1.5
Limit on BSM events $S_{obs}^{95} (S_{exp}^{95})$	$5.5 (5.5^{+2.1}_{-1.3})$	$12.4 (13.2^{+4.9}_{-3.5})$	$6.4 (5.2^{+2.6}_{-0.9})$
Limit on $(A\sigma)_{obs}^{95} ((A\sigma)_{exp}^{95})$ [fb]	$0.27 (0.27^{+0.11}_{-0.06})$	$0.61 (0.65^{+0.24}_{-0.17})$	$0.31 (0.26^{+0.13}_{-0.04})$
top only real τ_{had}	2.0 ± 1.1	8.2 ± 3.9	$0.2^{+0.3}_{-0.2}$
top ≥ 1 fake τ_{had}	0.9 ± 0.5	9.8 ± 4.5	$1.2^{+1.4}_{-1.2}$
W+jets	$0.01^{+0.02}_{-0.01}$	2.2 ± 0.6	0.4 ± 0.4
Z/ γ^* +jets	$0.04^{+0.15}_{-0.04}$	1.9 ± 1.1	-
t \bar{t} + V	0.04 ± 0.02	-	0.3 ± 0.1
Diboson	0.14 ± 0.02	-	-

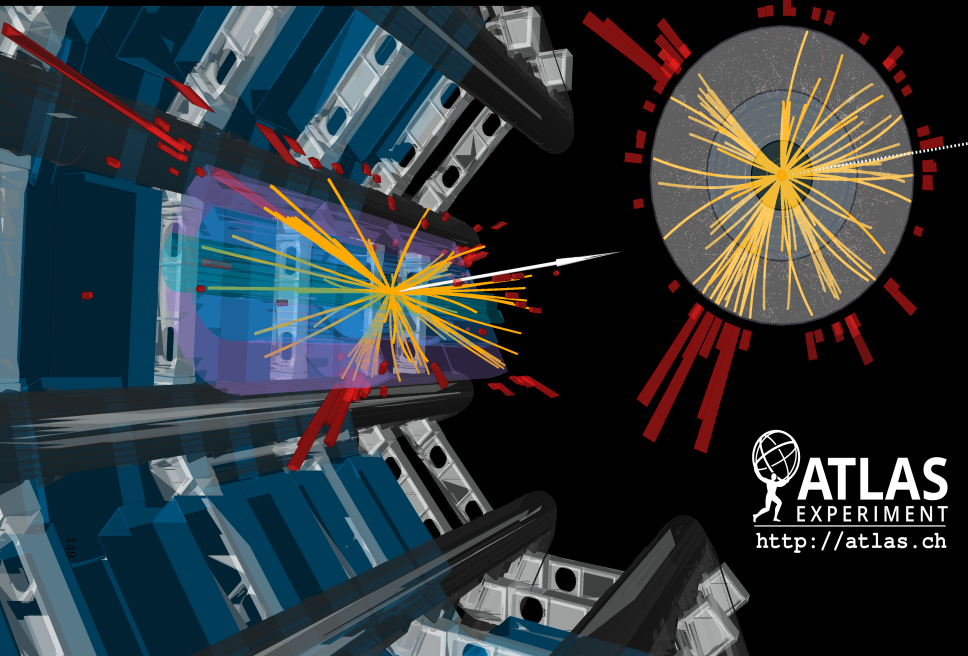
No excess over SM expectation has been found



Run: 209736

Event: 180956915

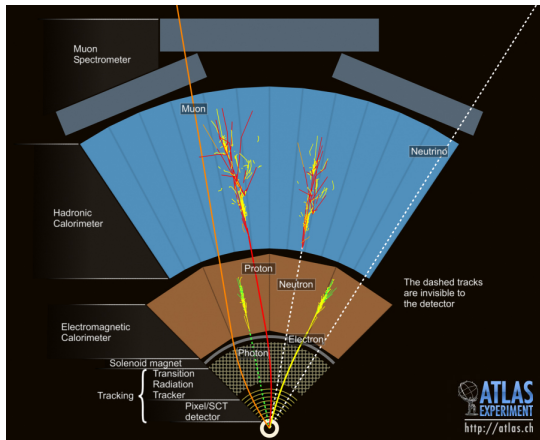
2012-09-04 05:56:10 CEST



 **ATLAS**
EXPERIMENT
<http://atlas.ch>

Event Reconstruction

- Outgoing particles leave different signatures in the sub-detectors
- Muons:
 - Combined **track** in Inner Detector and Muon Spectrometer
- Jets:
 - **Tracks** and EM/HAD calorimeter deposit
 - **Vertex reconstruction** for flavour tagging
- Electrons:
 - Bremsstrahlung corrected **tracking** and EM calorimeter deposit
- Photons:
 - EM deposit, but **tracking** and **vertex reconstruction** for conversions and **isolation**

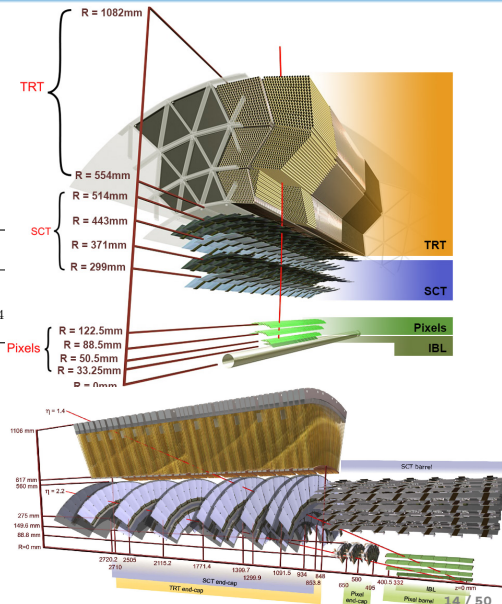
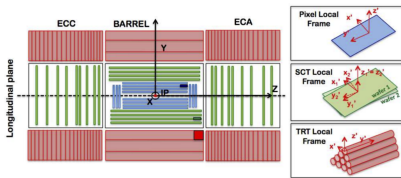


- Tracking is a fundamental ingredient for the reconstruction of every single high-level object candidate

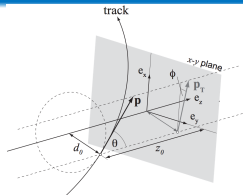
The ATLAS Inner Detector

- Axial 2T magnetic field
- 3 sub-detectors organised in Barrel and Endcaps
- **From 2014: Insertable B-Layer (IBL)**

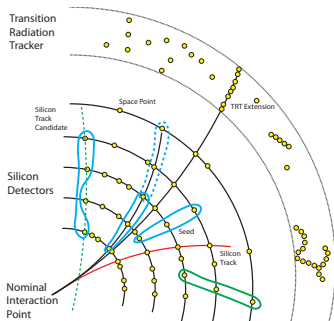
Subdetector	Element size	Intrinsic resolution [μm]	Radius barrel layers [mm]
IBL	$50 \mu\text{m} \times 250 \mu\text{m}$	8×40	33.2
Pixel	$50 \mu\text{m} \times 400 \mu\text{m}$	10×115	50.5, 88.5, 122.5
SCT	$80 \mu\text{m}$	17	299, 371, 443, 514
TRT	4 mm	130	from 554 to 1082



Track Reconstruction in ATLAS Inner Detector



Courtesy of A.Salzburger



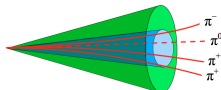
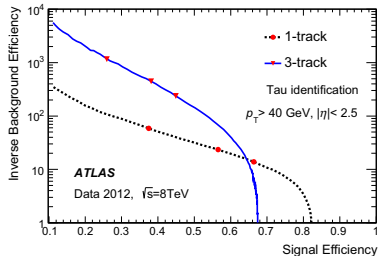
ATL-SOFT-PUB-2007-007

- Charged particles in magnetic field \rightarrow **helicoidal trajectory**
 $\tau = (d_0, z_0, \phi_0, \theta, q/p)$
- **Inside-out** algorithm for primaries:
 - Space points from detector hits
 - Identification of triplets of hits **seeds**
 - Adding measurements in outward layers via Kalman-Filter
 - **Ambiguity solver** to remove low-quality track-candidates
 - **From Run-2:** artificial neural networks to split shared hits *more on this later*
 - TRT extension for selected track-candidates and global- χ^2 fit
- **Outside-in** algorithm for secondaries:
 - Starting from TRT seeds and adding un-associated silicon hit from the **Inside-out** algorithm

From Tracks to Hadronic Taus

Hadronic Taus:

- Identification based on calorimeter and **tracking** information
- Combined in **two BDTs** for *1-prong* or *3-prong*
- Strong requirement on the identification robustness:
 $p_T \sim 10^1$ GeV \rightarrow $W, Z, \tilde{\tau}$
 $p_T \sim 10^2$ GeV \rightarrow SUSY Higgs search
 $p_T \sim 10^3$ GeV \rightarrow Z' search

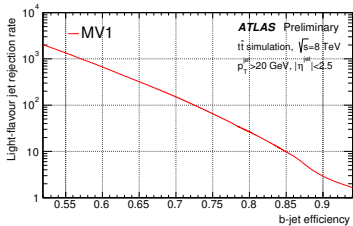
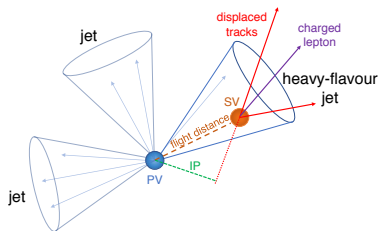
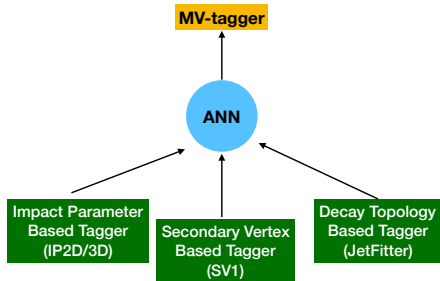


Variable	Offline	
	1-track	3-track
f_{cent}	•	•
f_{track}	•	•
R_{track}	•	•
$S_{\text{leadtrack}}$	•	
$N_{\text{iso track}}$	•	
ΔR_{Max}		•
$S_{\text{T}}^{\text{flight}}$		•
m_{track}		•
$m_{\pi^0+\text{track}}$	•	•
N_{π^0}	•	•
$p_{\text{T}}^{\pi^0+\text{track}} / p_{\text{T}}$	•	•

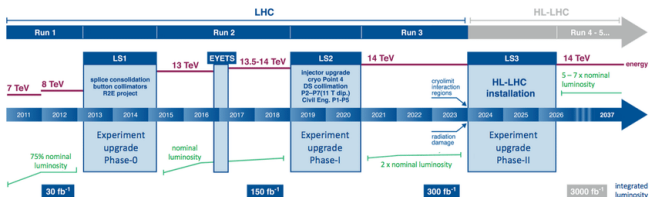
From Tracks to b-jets

B-Tagging:

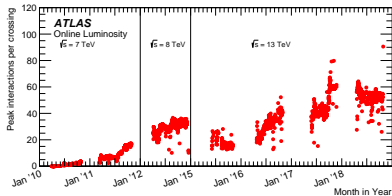
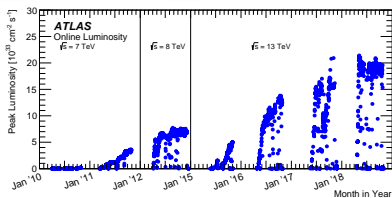
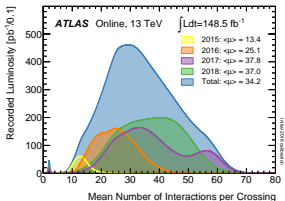
- The b-tagging algorithms are multivariate taggers
- Combine outputs from *low level* taggers into a single discriminant output
- Important to the *low level* d_0 resolution and secondary vertex reconstruction



From Run-1 to Run-2



- Design: $1 \times 10^{34} \text{ cm}^{-2}\text{s}^{-1}$ Run-2 record: $2.14 \times 10^{34} \text{ cm}^{-2}\text{s}^{-1}$ (May 16th 2018)
- Design: 19 <interactions/bc> Run-2: 37 <interactions/bc>



ATLAS Pixel Operation and Tracking Challenges

Pixel Detector:

- **Insertion of the new layer IBL**
 - Maintain Pixel performance with the B-Layer reaching the maximum dose
 - Closer layer to interaction point → improve d_0 , z_0 resolution
- Operate a detector in experimental conditions harsher than the design
- Counteract **Synchronisation errors, Radiation Damage, lower hit-on-track efficiency**

Tracking:

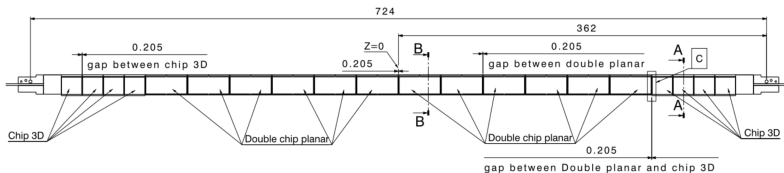
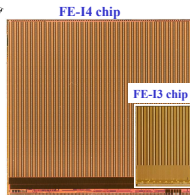
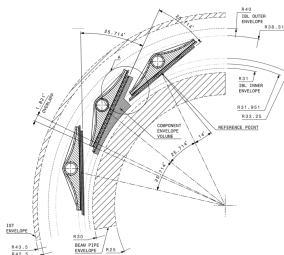
- Ensure high track reconstruction efficiency at high pile-up and low fakes
- **Update the alignment framework to include the IBL**
- **Improve tracking in dense environments**, i.e. when particles fly close to each other → lot of competitors for the same clusters

Hardware Upgrade

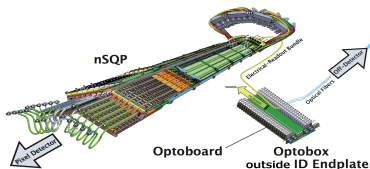
Hardware Upgrade

IBL in a nutshell

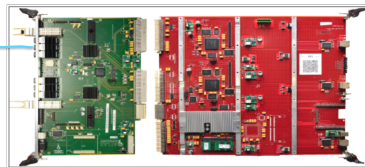
- Single pixel detector layer on a thinner new Beryllium beam-pipe (radius 29mm → 25mm)
- Closer to the interaction point
- Smaller pixel size: $50 \mu\text{m} \times 250 \mu\text{m}$
- IBL+beam pipe and structures: $< 2\% X_0$
- 14 staves length 72.4 cm, 1.82 degrees overlap in ϕ , no overlap in z, average radius 3.27 cm
- 12M readout channels
- Radiation hard up to $5 \times 10^{15} n_{eq}/\text{cm}^2$
- FEI4: 4-bit TOT, FEI3: 8-bit TOT



IBL Readout



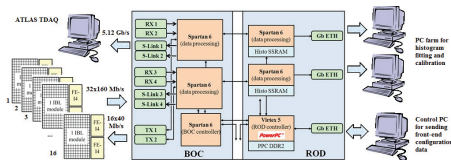
On-detector



Off-detector

Optical Fiber
70-90 m

- On-detector (as of 2014):
 - Readout per module at 80 Mbps (Ly2, Disks 1 and 3), 160 Mbps (others). Configuration at 40 Mbps
- **Off-Detector** (unified from 2018):
 - Back-of-crate cards (BOC) → Rx/Tx from/to modules, data output via S-Link to Readout system
 - Readout Drivers (ROD) → PowerPC, heavily used for configuration and monitoring,



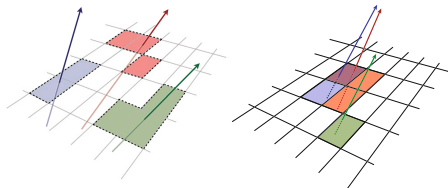
- User interface distributed over a private network which runs multithreading applications for **control, configuration, monitoring and user actions**

Reconstruction Software upgrade

Reconstruction Software upgrade

Tracking In Dense Environments

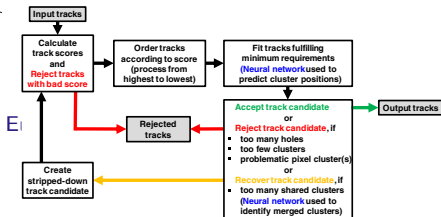
- In the core of energetic jets, or boosted hadronic τ , charged particles might have an angular separation smaller than the detector granularity
- **Shared measurements** \rightarrow worse position estimate / track-fit quality \rightarrow **track removal at ambiguity solver stage**



Phys. J. C 77 (2017) 673

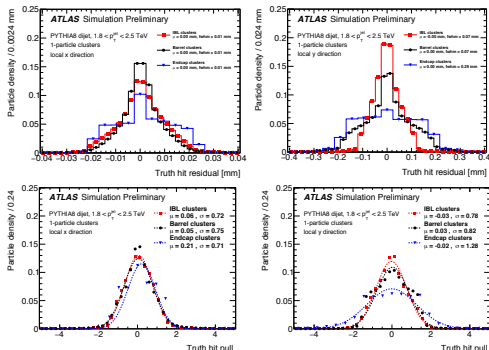
Neural Network and Combinatorial Filter:

- 3 sets of Neural Networks are used:
 - 1 for cluster splitting: 1,2 or >2 particles
 - 3 for X,Y position determination (for each class)
 - 6 for each direction uncertainty
 - Use of Combinatorial filter to associate every possible compatible cluster in a layer



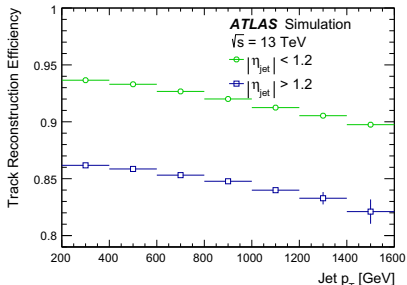
Tracking in Dense Environment - performance

- Neural Network position evaluate by reco-truth residual
- Unbiased residuals, errors



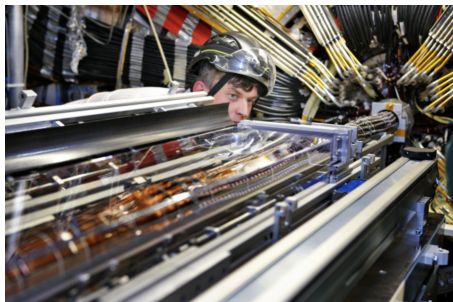
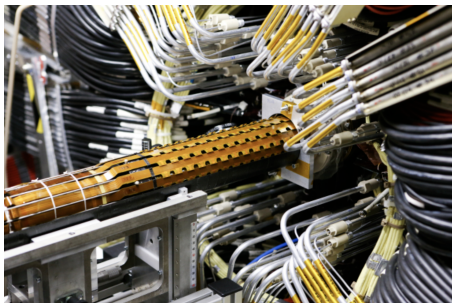
ATL-PHYS-PUB-2018-002

- Limitation due to the requirement of shared SCT clusters
- Reconstructible tracks: pass the SCT cluster requirement
- Recent work on SCT cluster splitting (backup)



Run-2 Commissioning

It's insertable indeed



But... how do we know if it has been properly placed?

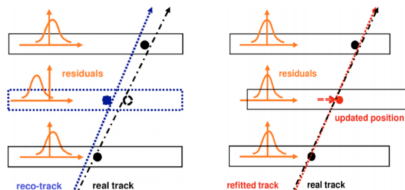
Photos by Claudia Marcelloni de Oliveira/CERN

Inner Detector Alignment

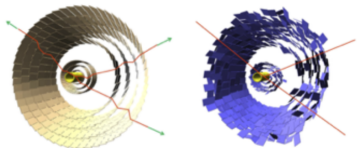
- **Concept:** Track fit worsened by **misplacement of sensitive element** wrt assumed geometry
- **Aim:** **Correct** the assumed geometry and determine the actual relative positions of all active elements

- **Track based technique** based on χ^2 minimisation
- $$\chi^2 = \sum_{hits} \left(\frac{m_i - h_i(\vec{\alpha})}{\sigma_i} \right)^2$$

 m_i measurements, h_i extrapolated hits, σ_i intrinsic resolution, $\vec{\alpha}$ align parameters
- Every alignment structure is assumed to be a **rigid body** with **6 Degrees of Freedom (DoF)**
 - **3 translations:** T_x, T_y, T_z
 - **3 rotations:** R_x, R_y, R_z



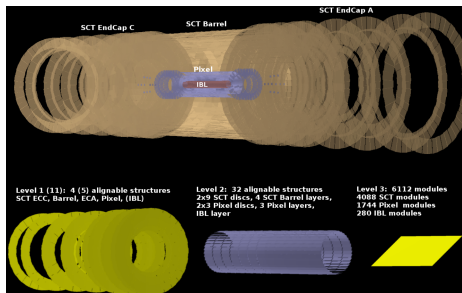
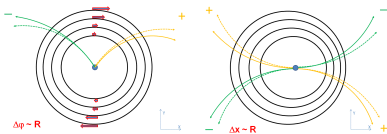
- Solve for small corrections iteratively



- Alignment is an iterative procedure, that adds corrections to a defined initial condition

ID Alignment Procedure

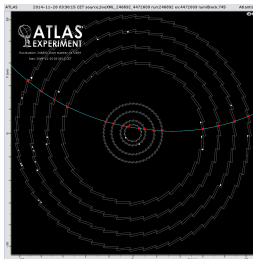
- Alignment procedure is split in **hierarchical levels** according to the mechanical structure of the detector:
 - Collective movements of full structures are corrected first
 - Single modules/wire alignment is the last step
- Weak Modes:** deformations that global χ^2 track-base alignment is insensitive to: **External constraints** to avoid reconstruction biases



Alignment level	Detector	Alignable Structure
Level 1/11	Pixel: barrel and end-caps	1
	IBL: layer (from Run-2)	1
	SCT: barrel and 2 end-caps	3
	TRT: barrel and 2 end-caps	3
	Total	7 (8 from Run-2)
Level 2	Pixel: barrel layers	3
	Pixel: end-caps disks	6
	IBL: layer (from Run-2)	1
	SCT: barrel layers	4
	SCT: end-cap disks	18
	TRT: barrel modules	96
	TRT: end-caps wheels	80
	Total	207 (208 from Run-2)
Level 3	Pixel: barrel modules	1456
	Pixel: end-caps modules	288
	IBL: modules	280
	SCT: barrel modules	2112
	SCT: end-caps modules	1976
	TRT: barrel wires	105088
	TRT: end-cap wires	245760
	Total:	356680 (356960 from Run-2)



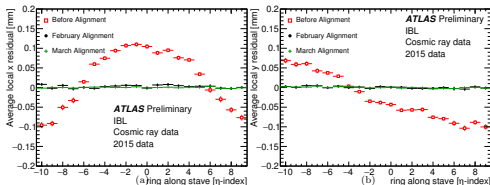
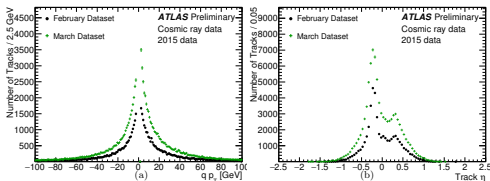
IBL Alignment Commissioning



- First alignment of the ATLAS ID after LS1 and IBL insertion
- Cosmic Ray Data → top-bottom tracks
- Systematic distortions observed:

- **local-y elongation:**
misplacement during gluing phase
- **local-x bowing in $r\phi$ direction:**
parabolic stave distortion

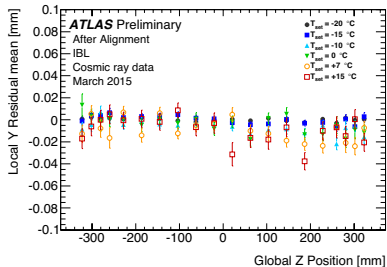
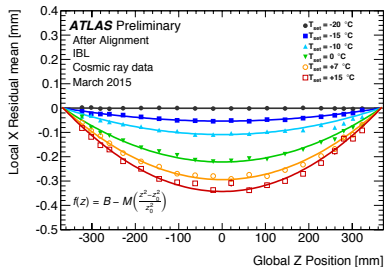
ATL-PHYS-PUB-2015-009, CERN-
THESIS-2017-380, Run2-EventDisplay



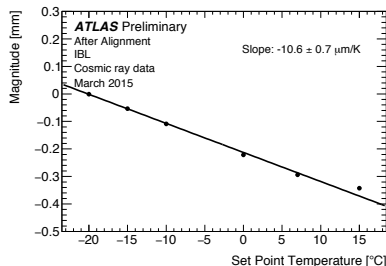
- Systematic distortions are corrected at Level3 alignment
- Not really a problem... as long as they are **static distortions**



Measurement of IBL Distortions using Cosmic Ray Data

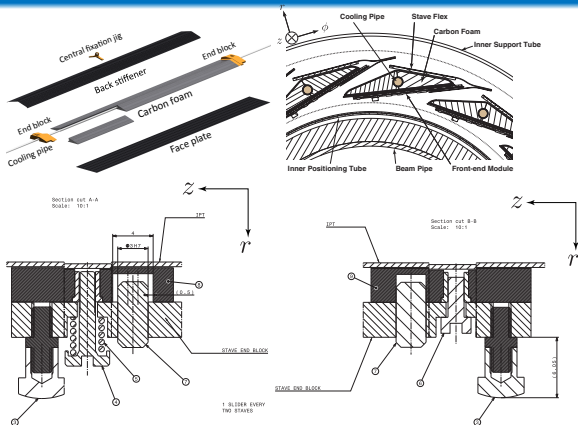


- Bowing dependence wrt operating temperature
- Hit-on-track residuals \rightarrow module position
- Distortion in $r\phi$, no change in z
- $r_x(z) = B + M\left(1 - \frac{z^2}{z_0^2}\right)$
 r_x = residual mean
 B, M = baseline (magnitude) of the distortion
 z_0 = fixing point

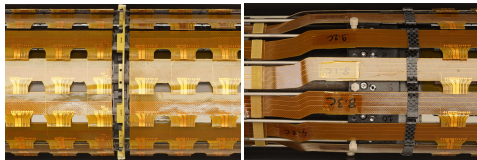


A step back and little bit more details..

- Staves with triangular cross section
- C-Side → screw, A-Side → pin (± 0.5 in z)
- **Coefficients of thermal expansion (CTE):**
 - Stave structure (carbon fibre): negligible
 - Stave flexible bus: ~ 30 ppm/K
- Mid-stave central right: constrain radial distortions



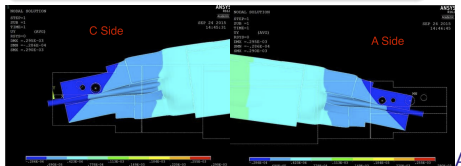
ATLAS-TDR-19, ATL-INDET-PUB-2015-001



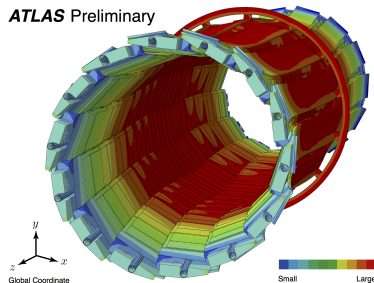
Finite element analysis results

IBL Bowing is due to:

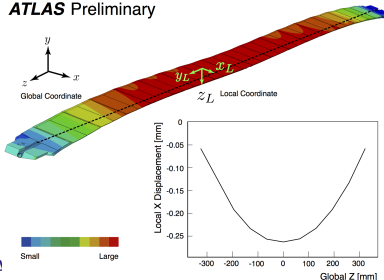
- CTE mismatch between the flex services and the carbon foam
- Mechanics of the fixed points of the staves:
 - The stave can rotate around the A-side pin
 - The C-side screw does not hold the distortion torque
- The non-uniform stave cross section due to the peek inserts at the fixed point
- Parabolic distortion predicted by FEA analysis



ATLAS Preliminary



ATLAS Preliminary



Impact on physics performance

- **Beam Spot:**

- Rotation, displacement and size (σ_x, σ_y) in transversal plane

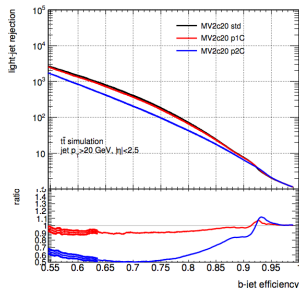
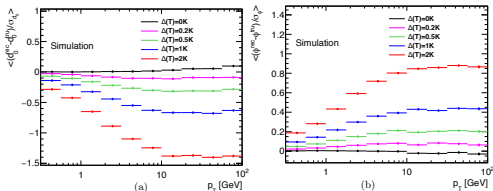
- **Track impact parameters:**

- Biased local- x residuals $\rightarrow d_0, \phi$ biases
- More significant for high- p_T tracks

- **B-Tagging:**

- Light-jet rejection decreases to 90% (50%) @ 70% wp for $\Delta T = 1\text{K}$ (2K)

ΔT [K]	$\sigma_{x,L}$ [μm]	$\sigma_{y,L}$ [μm]	$\sigma_{z,L}$ [μm]
0.0	13.9 ± 0.2	14.0 ± 0.2	53.3 ± 0.5
+0.2	13.9 ± 0.2	14.0 ± 0.2	53.3 ± 0.5
+0.5	14.1 ± 0.2	14.2 ± 0.2	53.3 ± 0.5
-1.0	14.3 ± 0.2	14.5 ± 0.2	53.3 ± 0.5
+1.0	14.5 ± 0.2	14.6 ± 0.2	53.3 ± 0.5
+2.0	16.9 ± 0.2	16.8 ± 0.2	53.3 ± 0.5



ATL-INDET-PUB-2015-001, CERN-THESIS-2017-380

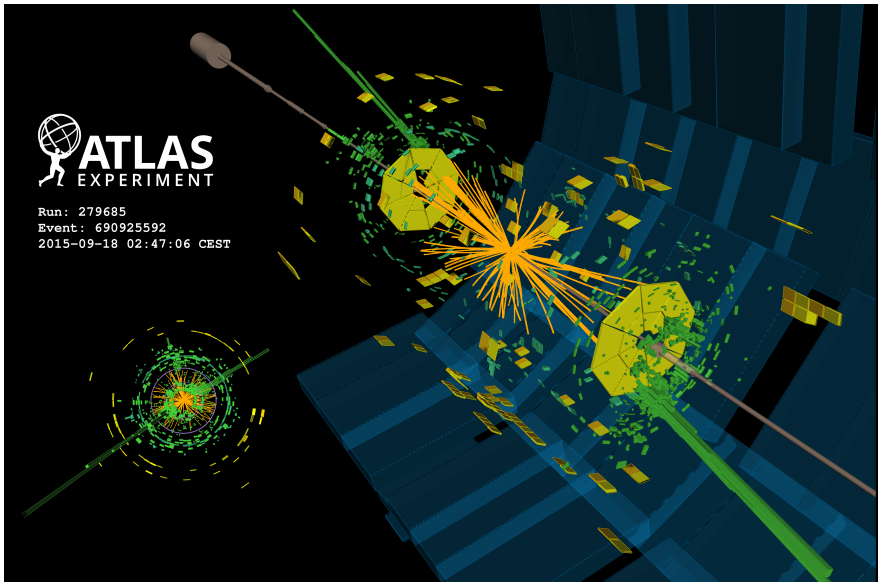


Temperature change $\Delta T < 0.2$ K is tolerable

Run-2 at $\sqrt{s} = 13$ TeV



Run: 279685
Event: 690925592
2015-09-18 02:47:06 CEST

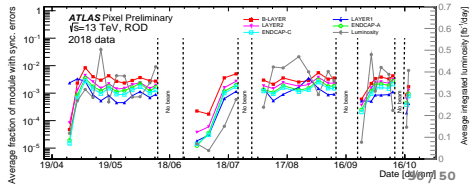
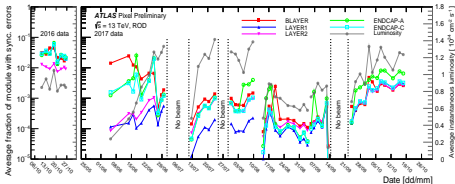
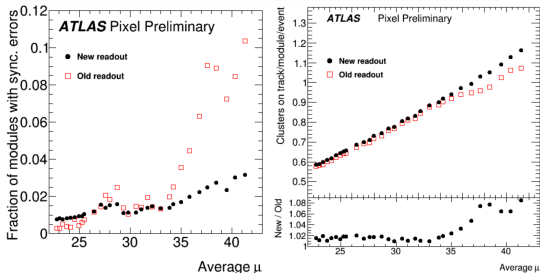


IBL and Pixel operation during Run-2

Figures of merit:

- **ROD synch Error:** mismatch between event-id information received from trigger and from module
- **MOD synch Error:** mismatch between event-id information received on the module from different FEs
- **Constant effort of Pixel DAQ team in deploying updated ROD FW** → keep de-synch stable with harsher conditions

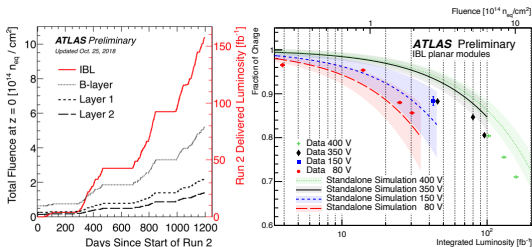
- Higher de-synch...
- ...lower N_{hits} on tracks...
- ...lower track quality and reconstruction efficiency



Average integrated luminosity [fb/day]

Radiation damage effect in Pixel and IBL

- Cope with radiation damage → significant for the detector performance
- Models are used to **understand and predict radiation damage effects**, which are now included in ATLAS MC simulation
- Will subdivide the radiation effects in two "**classes**"



Mid/Long time scale

- Over several data-taking runs
- **Charge Collection Fraction (CCF) reduction**
- Lorentz-Angle drift
- Depletion Voltage evolution
- **Counteract adjusting operational parameters**

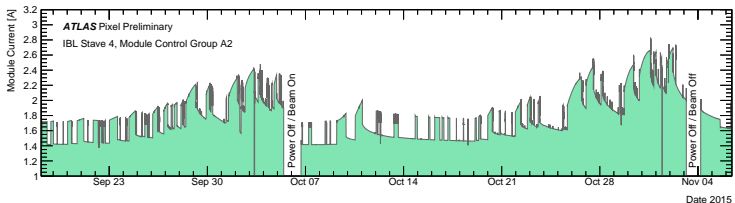
Short time scale:

- Effects apparent in each single run
- **LV current increase**
- **Detector detuning**
- **Single Event upsets and Single Event Transients**
- Require special counter actions → **dynamic detector evolution**

The radiation damage effects enlightened in bold will be discussed today

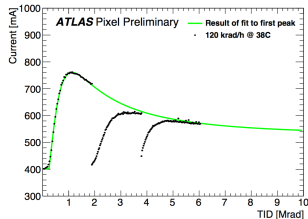
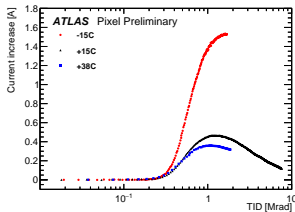


LV current increase: a hard start of Run-2



- Module current increase during operation starting from September 2015:

- **Within same data taking run:** up to $\Delta I \sim 0.5$ A
- **Continuous rise during operation:** up to $\Delta I \sim 1$ A
- **IBL switched OFF** due to voltage transients on supply devices



Total Ionizing Dose induced effect:

- FEs tested in lab with X-RAD iR160 X-Ray machine
- LV strongly dependent on dose/operating temperature
- Positive annealing when modules are powered off

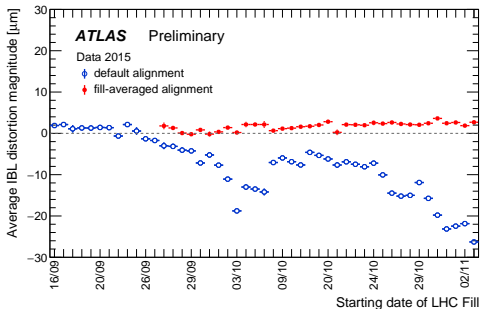
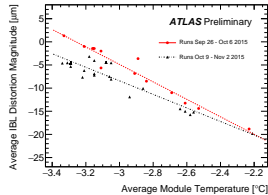
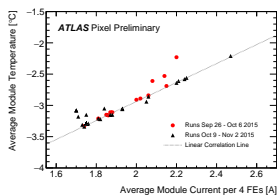
Effects on IBL distortion

Change in LV current \rightarrow Change in T_{mod} \rightarrow Change in T_{flex} \rightarrow IBL stave distortion

Not a static distortion:

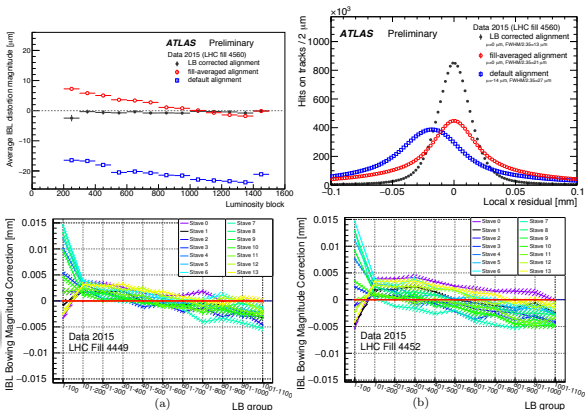
- Run-by-run and within run dependence
- L3 not feasible at prompt processing...
- ... but analytic description is known \rightarrow new single DoF M
- Simpler scheme: prompt-calibration is possible

Level 11							
Structure	T_x	T_y	T_z	R_x	R_y	R_z	M
TRT (Barrel)	✓	✓	✗	✓	✓	✓	✗
TRT (End-caps)	✓	✓	✗	✗	✗	✓	✗
SCT (Barrel)	Kept fixed as reference						
SCT (End-caps)	✓	✓	✗	✗	✗	✓	✗
Pixel	✓	✓	✓	✓	✓	✓	✗
IBL	✓	✓	✓	✓	✓	✓	✓
Level 16							
TRT	Kept Fixed as reference						
SCT	Kept Fixed as reference						
Pixel	Kept Fixed as reference						
IBL	✗	✗	✗	✗	✗	✗	✓



TID Effects on IBL distortion

- Developed a dynamic alignment **LB-group**^(*) wise
 - **Resolution improvement** wrt run-by-run alignment: $\sim \times 2$ FWHM: $21\mu\text{m} \rightarrow 13\mu\text{m}$
 - Same stave-by-stave evolution in agreement with constraining mid-stave ring...
- ...but why only from LB>100?

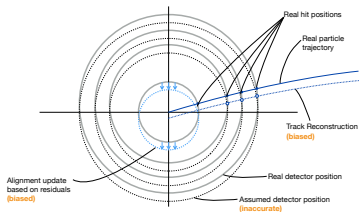


IDTR-2015-011, CERN-THESIS-2017-380

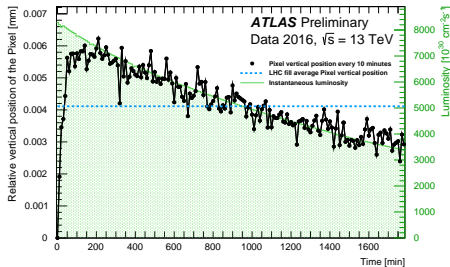
(*) A luminosity block (LB) is the amount of time during which the LHC conditions are approximately uniform, including (but not only) luminosity.



Dynamic Alignment Corrections of the ID



- Pixel package T_y vertical movement → due to coolant mass change over time
- If not corrected → artificial ϕ -dependent mis-alignment of IBL
- Speed of vertical drift follows delivered luminosity
- Other global movements T_x and T_z corrected as well (see backup)



Correcting short-time scale movements

- Excellent alignment accuracy
- Time-dependent re-alignment of full ID
- Within prompt calibration process
- Movements of $O(10\mu\text{m})$ for detector with resolution of $O(10\mu\text{m})$
- **Dynamic Alignment for full Run-2**

ID Alignment is NOT Pixel Alignment Only

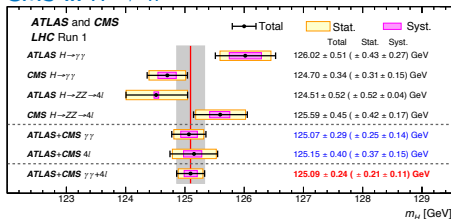
- What in the end matters is the combined alignment of Pixel+SCT+TRT
- ID Alignment *weak modes* can have a large impact on **momentum scale**, affecting precision measurements, i.e. m_H, m_W, \dots
- Proper modelling, timely correction

$$q/p_T \rightarrow q/p_T(1 + qp_T\delta_{sagitta})^{-1}$$

$$p_T \rightarrow p_T(1 + \delta_{radial})^2$$

	ΔR	$\Delta\phi$	ΔZ
R	Radial Expansion (distance scale) 	Curl (Charge asymmetry) 	Telescope (COM boost)
ϕ	Elliptical (vertex mass) 	Clamshell (vertex displacement) 	Skew (COM energy)
Z	Bowing (COM energy) 	Twist (CP violation) 	Z expansion (distance scale)

It's of paramount importance keeping ID systematics as low as possible. State of the art Run-1 alignment \rightarrow better momentum scale led to smaller syst wrt CMS in $H \rightarrow 4l$



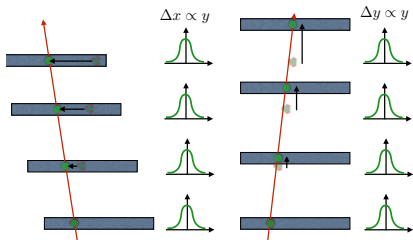
PRL114(19):191803

[η , η] range	[0,0, 0,8]		[0,8, 1,4]		[1,4, 2,0]		[2,0, 2,4]		Combined	
	p_T^c	m_T	p_T^c	m_T	p_T^c	m_T	p_T^c	m_T	p_T^c	m_T
Δm_W [MeV]										
Momentum scale	8.9	9.3	14.2	15.6	27.4	29.2	111.0	115.4	8.4	8.8
Momentum resolution	1.8	2.0	1.9	1.7	1.5	2.2	3.4	3.8	1.0	1.2
Sagitta bias	0.7	0.8	1.7	1.7	3.1	3.1	4.5	4.3	0.6	0.6
Reconstruction and isolation efficiencies	4.0	3.6	5.1	3.7	4.7	3.5	6.4	5.5	2.7	2.2
Trigger efficiency	5.6	5.0	7.1	5.0	11.8	9.1	12.1	9.9	4.1	3.2
Total	11.4	11.4	16.9	17.0	30.4	31.0	112.0	116.1	9.8	10.7

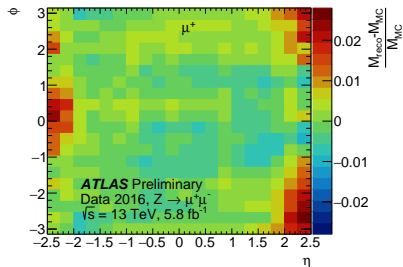
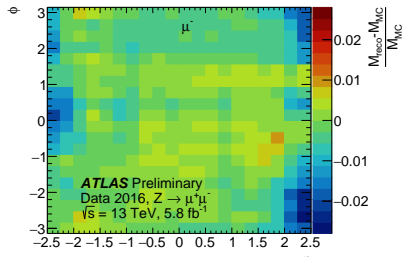
EPJC 78 (2018) 110



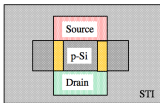
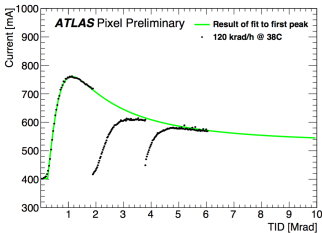
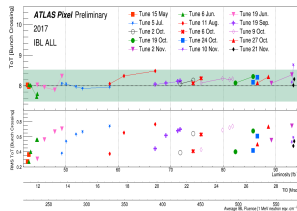
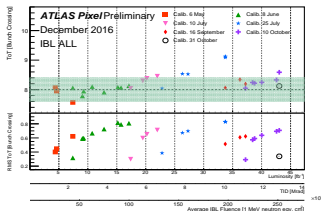
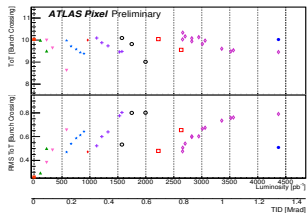
ID Alignment is **NOT** Pixel Alignment - Weak Modes



- Class of deformations leaving χ^2 unaffected, biasing track parameters
 - Need external constraints
- Charge dependent sagitta biases \rightarrow reconstructed momentum
- Use of Z mass from $Z \rightarrow \mu\mu$ and E/p ratio in $Z \rightarrow ee$ to constrain
- Impact parameters constrained by vertex position and $Z \rightarrow \mu\mu$ events



TID Effects on IBL Calibration

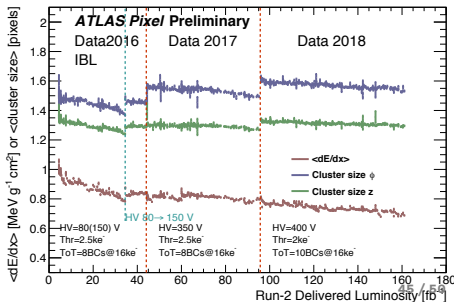
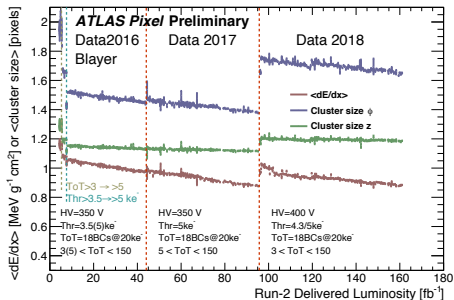


- Three effects occur in NMOS :
 - **positive charges** trapping in STI
 - e^- trapping in the Si-Si oxide interface
→ **permanent annealing**
 - e^- tunnelling at irradiation stop from Si substrate → **temporary annealing**
- Result:
 - Drift in opposite directions
 - **Continuous detector retuning**



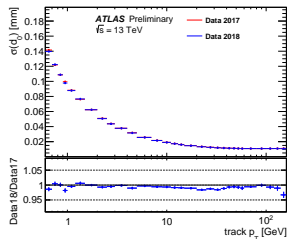
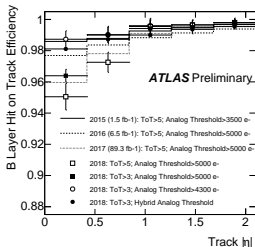
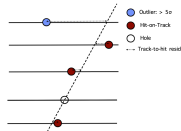
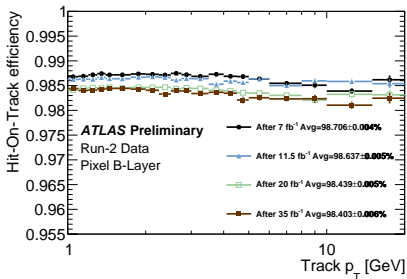
Mid/Long time scale effects: Charge Collection Fraction

- Major effect on IBL and B-Layer
- Clusters on tracks associated to jets $0.1 < \Delta R(trk, jet) < 0.4$
- Charge collection fraction loss, reduced cluster size \rightarrow expected **worsening of hit-resolution**
- **Constant efforts from operation team to maintain best possible detector performance:**
 - Bandwidth limitation in B-Layer in 2016 \rightarrow emergency tuning. Recovered in 2018.
 - Every few days \rightarrow retuning of IBL
 - HV change during operation \rightarrow recover full depletion
- **Anticipation** \rightarrow parameters resolution / LF-jets rejection degradation
Results not yet public.



Effects on hit-on-track efficiency and resolution

- CCF reduction + June 2016 emergency tuning: from 99% (2015) to 94% hit-on-track efficiency in $|\eta_{trk}| < 0.5$.
- Data 2018: Calibration software improvement for **first η dependent detector tuning**
 - Central η region \rightarrow lower threshold
 - High η region \rightarrow high threshold
 - **DAQ upgrade + FW improvements** \rightarrow $< 80\%$ bandwidth usage requirement
- Recovered cluster-size and hit-efficiency \rightarrow **improvement of d_0 resolution**



Short time scale effects: Single Event Upsets/Transients

Single Event Upset (SEU):

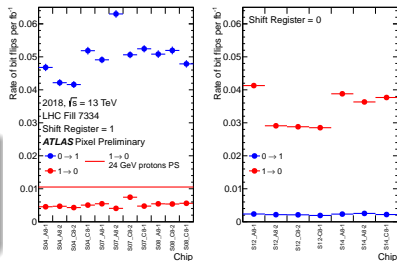
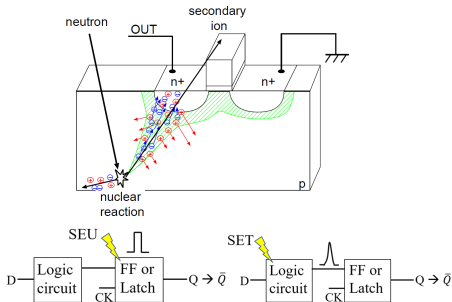
- A relevant amount of charge deposit into a memory latch **can flip its logic state**
- Highly ionizing recoil nuclei and showers from nuclear interactions of the MIPs

Single Event Transients (SET):

- Transient pulse caused by single event effect that propagates along the logic lines
- The last loaded configuration bitstream plays a role**

Memory corruption

- Developed read-back of module configuration \rightarrow corruption cross-section
- LHC data agrees with **test-beam** and FE simulation



Dynamic SEU/SET corrective actions

Joint effort between FW and SW:

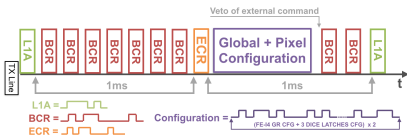
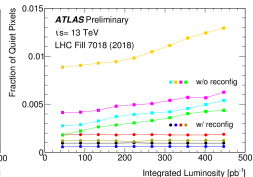
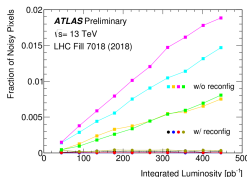
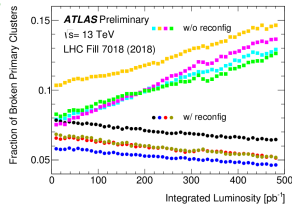
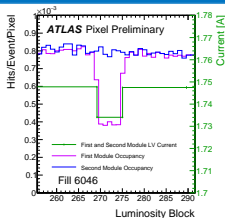
- Reconfiguration timed with ECR re-synchronisation signal
- In the shadow of the 0.02% of ATLAS dead time

Global Register Reconfiguration:

- In place from 2017 → fundamental to recover module operation

Pixel Register Reconfiguration:

- Tested in 2018 for the first time
- Not possible in *one go* → dynamic reconfiguration bitstream
- Noise, quiet pixels, broken cluster...



Anticipation of the ITK trickle

reconfiguration concepts.

Mandatory for Run-3 due to longer luminosity leveling time.

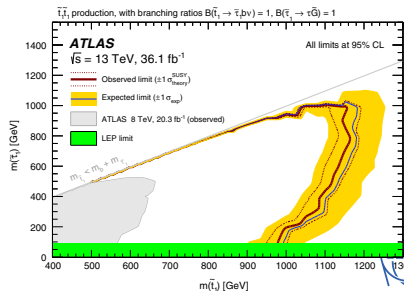
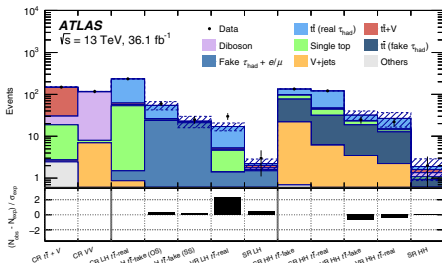
Full reconfiguration in 11 minutes



Back to physics analysis: $\tilde{t} \rightarrow \tilde{\tau}$ in Run-2

	CR HH $\tilde{t}\tilde{t}$ -fake	CR HH $\tilde{t}\tilde{t}$ -real	VR HH $\tilde{t}\tilde{t}$ -fake	VR HH $\tilde{t}\tilde{t}$ -real	SR HH
Charge(τ_1, τ_2)		opposite		opposite	opposite
$m_{T2}(\tau_1, \tau_2)$	< 30 GeV	< 30 GeV	[30, 80] GeV	[30, 80] GeV	> 80 GeV
$E_{\text{T}}^{\text{miss}}$	> 120 GeV	> 120 GeV	> 160 GeV	> 160 GeV	> 200 GeV
$m_{\text{T}}(\tau_1)$	< 70 GeV	> 70 GeV	< 100 GeV	> 100 GeV	
$m(\tau_1, \tau_2)$	> 70 GeV	> 70 GeV			

Variable	CR LH $\tilde{t}\tilde{t}$ -real	VR LH $\tilde{t}\tilde{t}$ -real	VR LH $\tilde{t}\tilde{t}$ -fake (OS)	VR LH $\tilde{t}\tilde{t}$ -fake (SS)	SR LH
Charge(ℓ, τ_{had})	opposite	opposite	opposite	same	opposite
$m_{T2}(\ell, \tau_{\text{had}})$	< 60 GeV	[60, 100] GeV	[60, 100] GeV	> 60 GeV	> 100 GeV
$E_{\text{T}}^{\text{miss}}$	> 210 GeV	> 210 GeV	> 150 GeV	> 150 GeV	> 230 GeV
$m_{\text{T}}(\ell)$	> 100 GeV	> 100 GeV	< 100 GeV		
$m(\ell, \tau_{\text{had}})$			> 60 GeV		



Wrap up: Pixel Operation Efforts Overview

- **Some of the Run-2 challenges:** guarantee optimal data acquisition at a Luminosity twice the original LHC (and Pixel) design and cope with radiation damage effects
- **Full ATLAS Pixel readout upgrade** to IBL readout type
- Pixel coped well with **Higher data rate** ensuring 98.9% of data acquisition efficiency in 2016, 100% in 2017 99.8% in 2018 thanks to ATLAS Pixel DAQ operation team
- Updates in **detector calibration software**
 - Improved SW stability for **frequent retuning** of IBL to correct for TID effects
 - Development of **η dependent tuning** which led to hit-on-track efficiency for B-Layer >98% despite radiation damage
- **Timely Firmware updates** to cope with ROD/MOD desynchronisation → stable at a rate of 10^{-3} despite 2018 harsher conditions
- Measurement of **SEU/SET** and development of **dynamic reconfiguration** for Run-3 → recovers up to 30% noise occupancy and ~ 2% quiet pixels



Wrap up: Tracking and Alignment efforts Overview

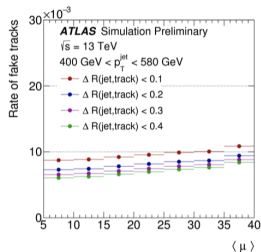
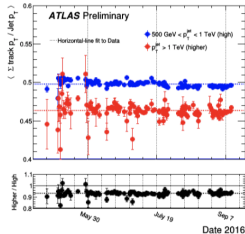
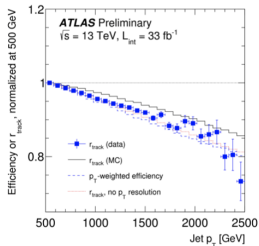
- **Some of the Run-2 challenges:** recover track reconstruction inefficiency in dense environment and correct for short time scale detector movements
- Development of **dynamic alignment corrections** to correct for TID induced IBL bowing and global movements of Pixel detector → resolution improved of factor x2 in IBL
- Correction of ID alignment **weak modes** during Run-2 to ensure reduction of ID systematics → sagitta biases $< 0.1 \text{ TeV}^{-1}$
- Pixel **Neural Network** pixel clustering and **restructure of Ambiguity solver** steps → recovery of track efficiency in dense jet-cores: $\sim 6\%$ of tracks are lost (see backup)

(Personal) Conclusions

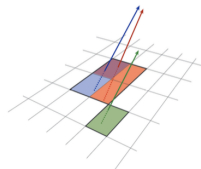
- **Run-2 was particularly challenging for ATLAS Pixel**, both in terms of detector operation and alignment
- The work performed in the areas of **DAQ, detector operation, tracking performance and alignment** is beneficial for the excellent performance of the object reconstruction algorithms → **important contribution for every analysis of the ATLAS Collaboration**
- The **expertise** gained working in this field is **transferrable to other scenarios** as the basic **tools and concepts are common** amongst different HEP experiments

BACKUP

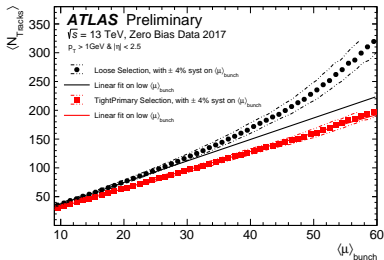
Dense Environment Performance



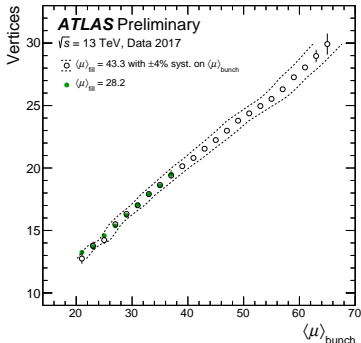
- Carefully monitor tracking performance in dense environments, such as jet cores
 - Lose efficiency due to highly collimated tracks sharing many clusters - Mitigated by using Neural Networks to identify clusters which can be shared without penalty
- Keep good efficiency while fake rate remains mostly below 1%, despite very dense environment



General Track Performance



- Reconstruct tracks above 500 MeV
- Provide two working points depending on needs
 - Loose for higher efficiency
 - TightPrimary for higher purity
 - Differ in hit-on-track requirements



Loose :

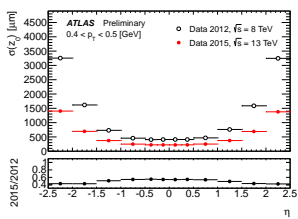
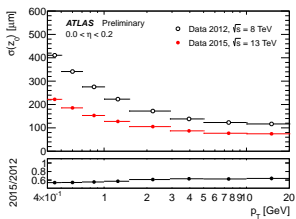
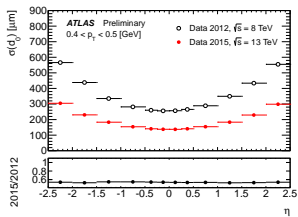
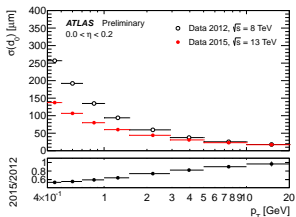
$|\eta| < 2.5$
Number of Silicon Hits ≥ 7
Number of Shared Modules ≤ 1
Number of Silicon Holes* ≤ 2
Number of Pixel Holes ≤ 1

Tight:

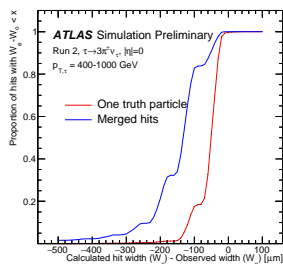
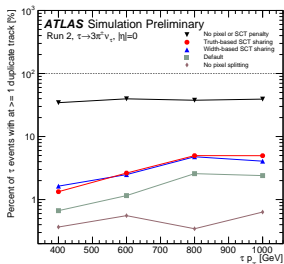
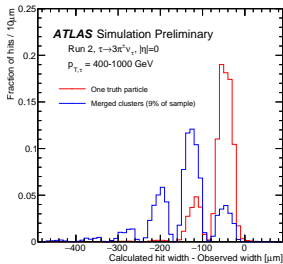
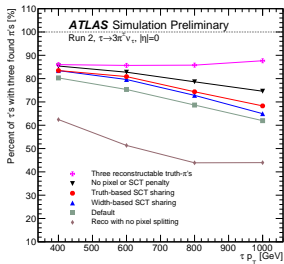
Number of Silicon Hits ≥ 9 (11 for $|\eta| > 1.65$)
At least 1 Hit on first two pixel layers (if expected)
No pixel Holes



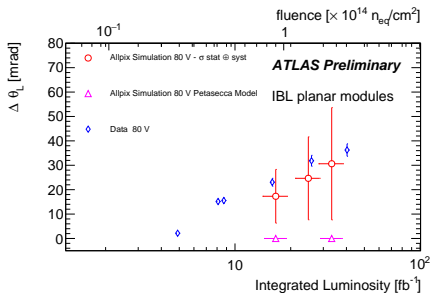
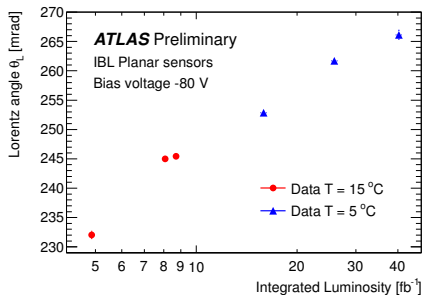
Impact of IBL



SCT Cluster Splitting



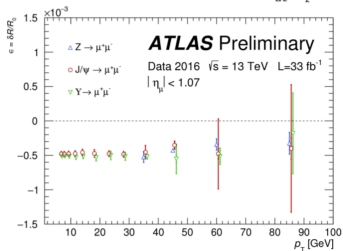
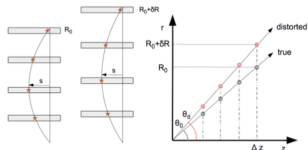
Lorentz Angle



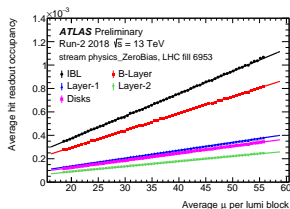
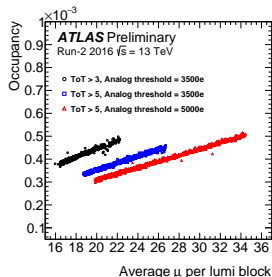
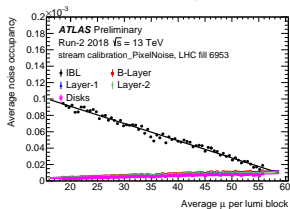
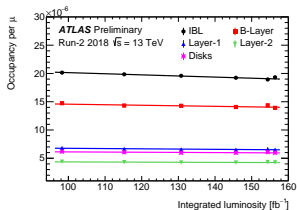
Radial Distortions

Recent precision alignment studies observed effect consistent with radial expansion of Inner Detector barrel

- -0.1% absolute scale correction, corresponds to 250 μm shift of SCT outer barrel layer
- Can be result of genuine mechanical effect, or consequence of alignment procedure
- Correcting such an effect would bring significant advantages, especially for precision SM measurements (e.g. W and Z mass)
- Allow J/ψ -based momentum calibrations with significantly reduced statistical uncertainty compared to current Z -based calibration



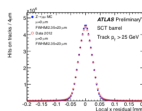
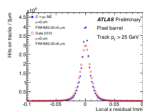
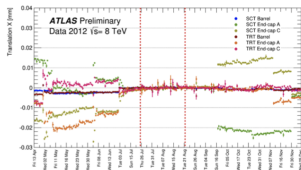
Hit Occupancies



Run1 align state of the art

Level	Description	Structures	DoF	Constraints
1	Pixel detector kept fixed			
	SCT split into barrel and 2 end-caps	3	All	
	TRT split into barrel and 2 end-caps	3	All except T_z	
2	Pixel barrel split into layers	3	All	
	Pixel end-caps split into disks	6	T_x, T_y, R_z	Beam spot,
	SCT barrel split into layers	4	All	Momentum bias and
	SCT end-caps split into disks	18	T_x, T_y, R_z	Impact parameter bias
	TRT split into barrel and 2 end-caps	3	All except T_z	
Si 3	Pixel barrel modules	1456	All	
	Pixel end-caps modules	288	T_x, T_y, R_z	Beam spot,
	SCT barrel modules	2112	All	Momentum bias and
	SCT end-caps modules	1976	T_x, T_y, R_z	Impact parameter bias
	TRT barrel split into barrel modules	96	T_x, T_y, R_z	Module placement accuracy
	TRT end-caps split into wheels	80	T_x, T_y, R_z	
TRT 3	Pixel and SCT are fixed			
	TRT straw level	351k	T_x, R_z	

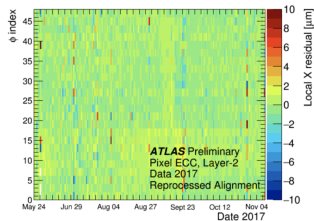
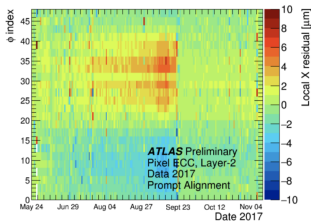
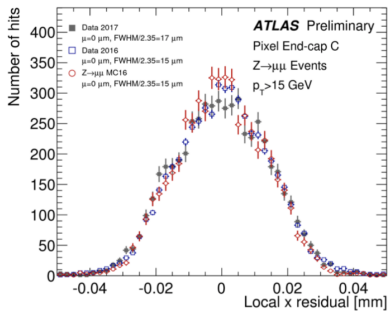
- Comparison between unbiased residuals in data to those of perfectly aligned MC simulation
- Alignment at μm level
- Correction of p_T, d_0 biases
- ID subdetectors movement monitored run by run basis



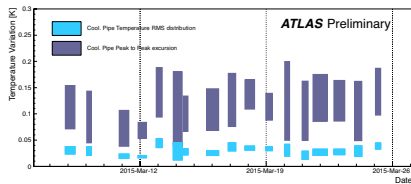
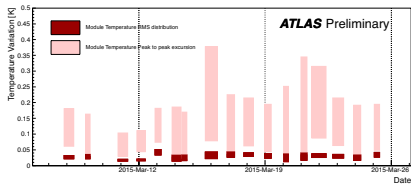
ATLAS-CONF-2014-047



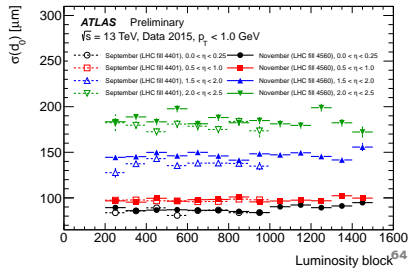
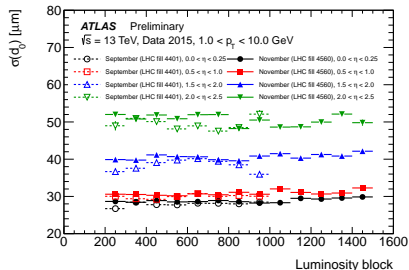
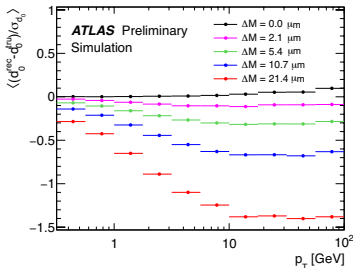
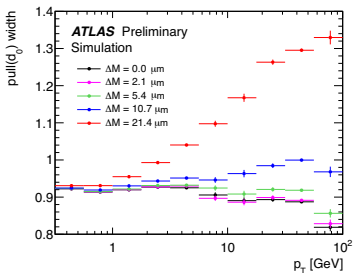
Recent align results



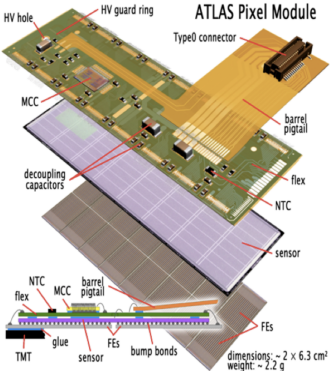
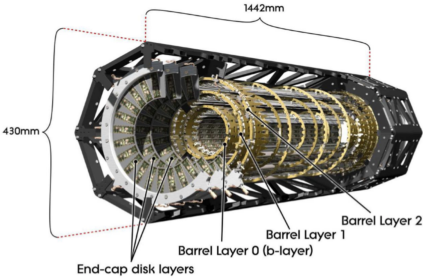
Temperature stability during Cosmic Ray Data



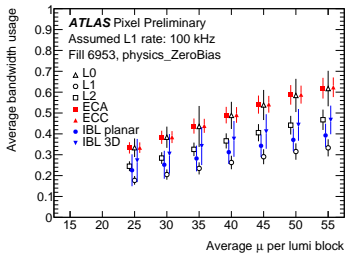
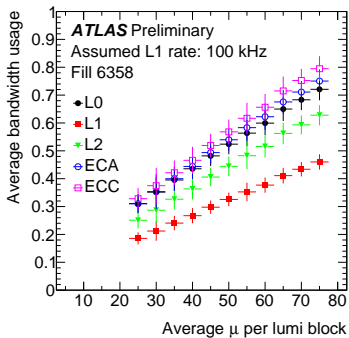
Effect of Bowing distortion and Dynamic Bowing correction on track parameters



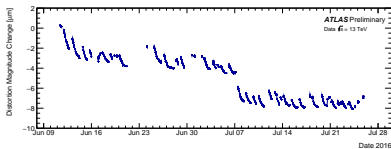
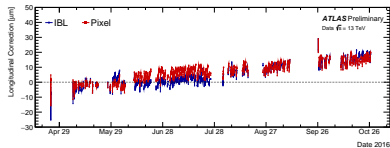
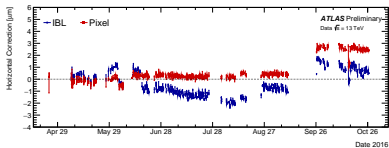
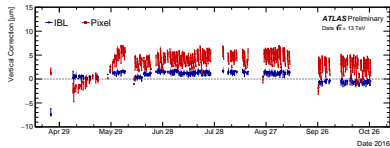
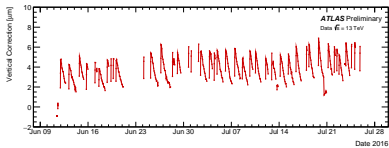
Pixel Detector



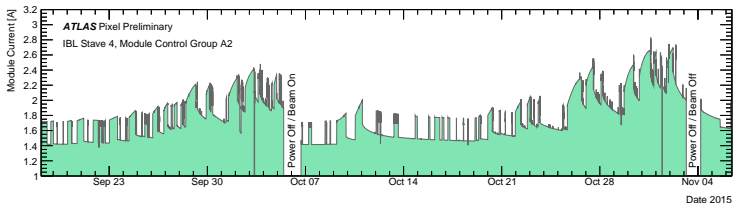
Bandwidth usage (2017 left, 2018 right)



More results of alignment dynamic corrections



Data 2015 inefficiency due to IBL switch off



ATLAS pp 25ns run: August-November 2015

Inner Tracker			Calorimeters		Muon Spectrometer				Magnets	
Pixel	SCT	TRT	LAr	Tile	MDT	RPC	CSC	TGC	Solenoid	Toroid
93.5	99.4	98.3	99.4	100	100	100	100	100	100	97.8

All Good for physics: 87.1% (3.2 fb⁻¹)

Luminosity weighted relative detector uptime and good data quality (DQ) efficiencies (in %) during stable beam in pp collisions with 25ns bunch spacing at $\sqrt{s}=13$ TeV between August-November 2015, corresponding to an integrated luminosity of 3.7 fb⁻¹. The lower DQ efficiency in the Pixel detector is due to the IBL being turned off for two runs, corresponding to 0.2 fb⁻¹. Analyses that don't rely on the IBL can use those runs and thus use 3.4 fb⁻¹ with a corresponding DQ efficiency of 93.1%.



Phenomenology of GSMB

$$\bar{d} = \left(\frac{100 \text{ GeV}}{m_{\tilde{\tau}}} \right)^5 \left(\frac{\sqrt{F/k}}{100 \text{ TeV}} \right)^4 \sqrt{\frac{E^2}{m_{\tilde{\tau}}^2} - 1} \times 10^{-2} \text{ cm.}$$

- if $\sqrt{F/k} > 10^6$, stable $\tilde{\tau} \rightarrow dE/dx$ searches
- if $\sqrt{F/k} \sim 10^6$ measurable decay length \rightarrow displaced vertex searches
- if $\sqrt{F/k} < 10^6$ prompt decay \rightarrow final state with τ particles

Track reconstruction efficiency

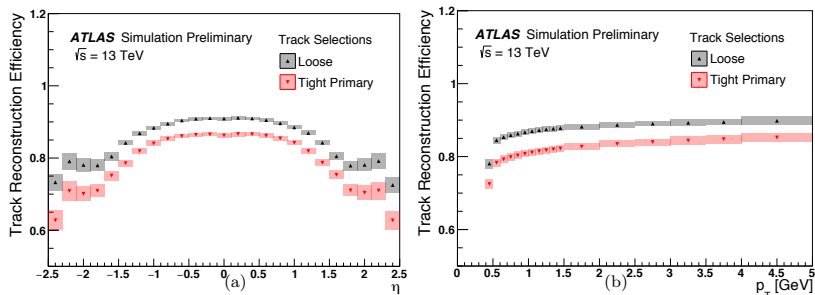
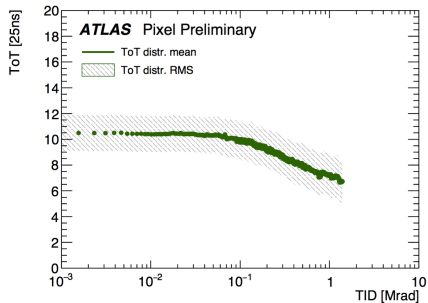
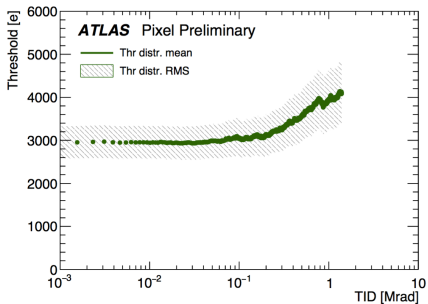
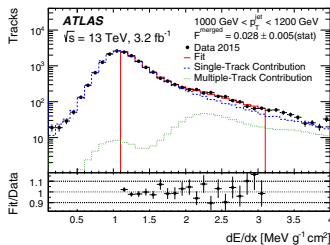
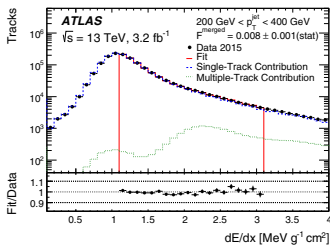


Figure 3.2: Track reconstruction efficiency measured on a PYTHIA [126] Minimum Bias [127] MC simulation [128] as a function of η (a) and p_T (b). The error bands represent the total systematic uncertainty. *Loose* indicate the default Run-1 selection. For (a) $p_T > 400$ MeV and for (b) $|\eta| < 2.5$ requirements are applied.

Variable	Description
Central energy fraction f_{cent}	Ratio between the E_T deposited in the region $\Delta R < 0.1$ and all energy deposited in the region $\Delta R < 0.2$ around the direction of the τ_{had}
Leading track momentum fraction (f_{track})	Ratio between the p_T of the leading track and the total transverse energy in the core region of a τ_{had}
Track radius (R_{track})	p_T -weighted distance of the associated tracks to the τ_{had} direction
Leading track d_0 significance ($S_{\text{leadtrack}}$)	Ratio between the transverse impact parameter of the leading track in the τ_{had} core region with respect to the TV and its estimated error
Number of tracks in the isolation region $N_{\text{track}}^{\text{iso}}$	Number of tracks associated with τ_{had} within $0.2 < \Delta R < 0.4$
Maximum ΔR	Maximum ΔR between an associated track to the τ_{had} candidate and the τ_{had} direction
Transverse flight path significance (S_T^{flight})	The decay length of the secondary vertex in the transverse plane with respect to the TV. Only for multi-track τ_{had} .
Track mass (m_{track})	Invariant mass calculated by the four-momenta of the tracks associated to the core region of a τ_{had}
Track-plus- π^0 -system-mass ($m_{\pi^0+\text{track}}$)	Invariant mass of the system composed by the tracks and π^0 reconstructed in the core region of τ_{had}
Number of π^0 's N_{π^0}	Number of π^0 mesons reconstructed in the core region
Ratio of tracks-plus- π^0 -system p_T ($p_T^{\pi^0+\text{track}}/p_T$)	Ratio between the p_T of the τ_{had} estimated using tracks and reconstructed π^0 and the calorimeter-only measurement



F-Lost

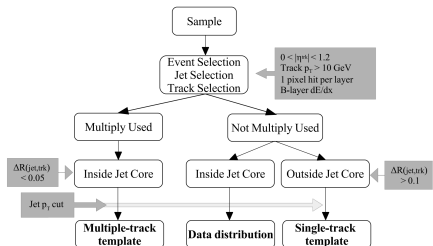


$$F^{\text{lost}_2} = \frac{N_{\text{Lost}}}{N_2^{\text{True}}}$$

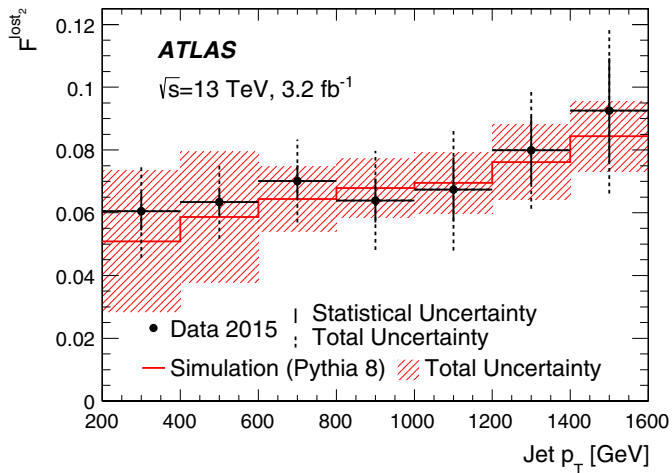
$$\approx \frac{N_{\text{Lost}}}{N_2^{\text{Reco}} + 2 \cdot N_{\text{Lost}}}$$

where

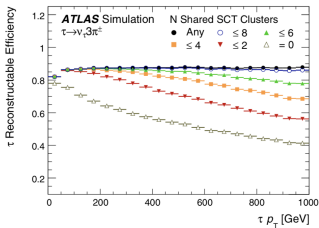
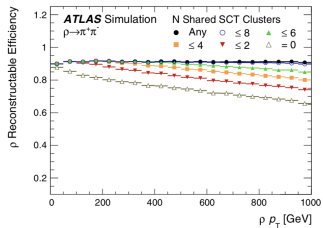
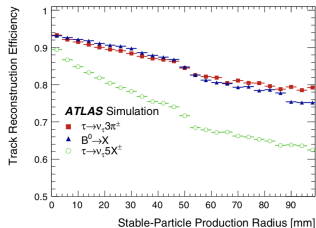
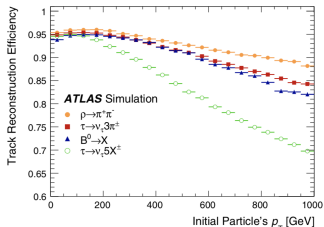
$$N_{\text{Lost}} = F^{\text{merged}} \cdot N_{\text{Data}}^{\text{Reco}}$$



F-Lost 2



Dense Environment performance



IBL BTagging

